Available online at www.sciencedirect.com
ScienceDirect
Life Sciences 81 (2007) 1031 – 1041
Life Sciences
www.elsevier.com/locate/lifescie

Expression of striatal adenosine and dopamine receptors in mice deficient in the p50 subunit of NF-κB

Xiaobin Xie, Krishna A. Jhaveri, Ming Ding, Larry F. Hughes, Linda A. Toth *, Vickram Ramkumar

Department of Pharmacology, Southern Illinois University School of Medicine, PO Box 19629 Springfield IL 62794-9629, United States

Received 10 May 2007; accepted 20 July 2007

Abstract

The striatal dopamine D2 receptor (D2R) and adenosine A2A receptor (A2AAR) exhibit mutually antagonistic effects through physical interactions and by differential modulation of post-receptor signaling pathways. The expression of the A2AAR and the D2R is differentially regulated by nuclear factor-κB (NF-κB). In this report, we determined the role of NF-κB in regulation of these receptors by comparing mice deficient in the NF-κB p50 subunit (p50 KO) with genetically intact B6129PF2/J (F2) mice. Quantification of adenosine receptor (AR) subtypes in mouse striatum by real time PCR, immunocytochemistry and radioligand binding assays showed more A2AAR but less A1AR in p50 KO mice as compared with F2 mice. Striata from p50 KO mice also had less D2R mRNA and [^{3}H]-methylspiperone binding than did striata from F2 mice. $G_{\alpha olf}$ and $G_{\alpha s}$ proteins, which are transducers of A2AAR signals, were also present at a higher level in striata from the p50 KO versus F2 mice. In contrast, the $G_{\alpha i1}$ protein, which transduces signals from the A1AR and D2R, was significantly reduced in striata from p50 KO mice. Behaviorally, p50 KO mice exhibited increased locomotor activity relative to that of F2 mice after caffeine ingestion. These data are consistent with a role for the NF-κB in the regulation of A1AR, A2AAR, D2R and possibly their coupling G proteins in the striatum. Dysregulation of these receptors in the striata of p50 KO mice might sensitize these animals to locomotor stimulatory action of caffeine.
© 2007 Elsevier Inc. All rights reserved.

Keywords: Adenosine; Dopamine; Receptor; Mice; Knockout; Locomotor activity

Introduction

Adenosine produces physiologic effects by activating different adenosine receptor (AR) subtypes (Dunwiddie and Masino, 2001). The A1AR subtype is widely distributed in the brain, with high concentrations in the hippocampus and cortex. In contrast, the A2AAR is localized primarily in the striatum (Riberio et al., 2002). The expression of ARs is differentially regulated by the transcriptional factor nuclear factor-κB (NF-κB). For example, oxidative stress induces A1AR expression through activation of NF-κB (Nie et al., 1998), while activation of NF-κB reduces A2AAR expression (Nie et al., 1999). A2AAR activation leads to inhibition of NF-κB (Majumdar and Mallick, 2003) (Sands et al., 2004). Furthermore, activation of NF-κB increases D2R expression (Fiorentini et al., 2002). These relationships suggest that striatal adenosine and dopamine signaling could be regulated by NF-κB.

NF-κB functions as either a homo- or heterodimer comprised of two functional subunits, p50 and p65. In their inactive state, the homo- or heterodimers are localized to the cytosol where they are associated with IκB. Activation of NF-κB involves phosphorylation of IκB by IκB kinase, followed by ubiquitination and translocation to the nucleus. The p50–p65 heterodimer and p65–p65 homodimers are transcriptional activators, while p50–p50 homodimers generally inhibit transcription (Karin and Ben-Neriah, 2000). The p50 subunit facilitates the binding of the p65 subunit to DNA to facilitate transcription. Cultured neurons from striatum (Yu et al., 2000) and hippocampus (Yu et al., 1999) of p50 KO mice exhibit enhanced oxidative stress and increased cell death upon neuronal excitotoxin challenges, thus suggesting a role of p50 subunit in homeostasis in central nervous system. Genetic deletion of the p65 subunit of NF-κB results in embryonic lethality (Beg et al., 1995), but mice that

* Corresponding author. Southern Illinois University School of Medicine, Box 19616, Springfield, IL 62794-9616, United States. Tel.: +1 217 545 7936; fax: +1 217 545 7273.
E-mail address: ltoth@siumed.edu (L.A. Toth).

0024-3205/$ - see front matter © 2007 Elsevier Inc. All rights reserved.
doi:10.1016/j.lfs.2007.07.031

lack the p50 subunit survive and are fertile (Sha et al., 1995), providing an animal model of altered NF-κB function.

The striatum is an ideal brain region for studying interactions among the A1AR, A2AAR and D2R and their regulation by NF-κB. Striatum has a high content of A2AAR (Rosin et al., 2003), and A2AAR and D2R co-localize on GABAergic striatopallidal neurons, where they mediate reciprocal inhibitory actions (Xu et al., 2005). The latter relationship is also supported by an *in vitro* study showing differential effects on adenylyl cyclase between the A2AAR and D2R (Hillion et al., 2002).

In this study, we assessed the effect of genetic deletion of the p50 subunit of NF-κB p50 (p50 KO) on expression of A1AR, A2AAR and D2R in mice. The data show enhanced A2AAR, $G_{\alpha s}$ and $G_{\alpha olf}$ proteins, but reduced D2R, A1AR expression and $G_{\alpha i}$ proteins in p50 KO mice as compared with F2 mice. Behaviorally, p50 KO exhibited enhanced locomotor activity to in response to oral administration of caffeine.

Materials and methods

Experimental animals

Four week old male B6;129P2-Nfkb1 mice (p50 KO) and B6129PF2/J mice (F2, the recommended control strain) were purchased from Jackson Laboratory (Bar Harbor, ME). Mice were housed by strain in groups of 2 or 4 per cage, and were used experimentally at 8 weeks of age. Cages were maintained at 22±1 °C on a 12:12 h light:dark cycle. Food and water were available *ad libitum*. Some F2, p50 KO and heterozygous p50 KO mice were bred in our animal facility and euthanized for tissue collection at 1, 4, and 8 weeks of age. The Laboratory Animal Care and Use Committee at Southern Illinois University School of Medicine approved all animals and experimental procedures used in this study.

Behavioral studies

Separate groups of p50 KO and F2 mice ($n=14$ per group) were used for behavioral assessment. Mice were anesthetized by subcutaneous injections of mixture of ketamine (50 mg/kg) and xylazine (50 mg/kg), and were surgically implanted with intraperitoneal abdominal transmitters (Transoma Medical, St. Paul, MN) to telemetrically quantify locomotor activity. After surgery, mice were housed in individual cages in a sound shielded chamber under a 12:12 h light:dark cycle (9:00 am to 9:00 pm) at 22±1 °C, and allowed 14 days for surgical recovery. Ibuprofen (0.2 mg/mL) was provided in drinking water from 1 day before through 5 days after surgery to provide analgesia.

After a minimal 2 week period to recover from surgery, mice of both strains were randomly assigned into caffeine treatment or control groups ($n=14$ per group). Data collection was initiated at light onset after the end of post-surgical recovery period. Mice received sequentially regular drinking water for 48 h (baseline), sucrose (20 g/L) only in drinking water for the next 48 h, and caffeine (300 mg/L) with sucrose for the final 96 h. Control mice received sucrose alone in drinking water. Caffeine intake per 24 h was 101±6 mg/kg for F2 mice and 107±4 mg/kg for p50 KO mice ($p>0.05$). Mice were euthanized 96 h after initiation of caffeine availability. Striatum was removed and stored at −80 °C until further use.

The frequencies emitted by the intraperitoneal transmitter were received by a DSI receiver (RPC-1) positioned under each individual animal cage. Collected signals were processed through a DSI analog converter. The locomotor activity was detected as transmitter movement across the receiver and recorded as number of movement events per min. Locomotor activity values were summed across 10 min intervals, and then averaged for every 2 h interval across the entire recording period. Data collected during the 2-day baseline and sucrose segments of the study were compared data obtained on each of the 4-days period of caffeine administration.

Membrane preparation

Striata were thawed in ice-cold 50 mM Tris–HCl buffer (pH 8.25 at 4 °C) that contained 10 mM $MgCl_2$, 1 mM EDTA, 10 μg/mL soybean trypsin inhibitor, 10 μg/mL benzamidine, and 2 μg/mL pepstatin (buffer A). Tissues were then homogenized by sonication for 6–8 s, and were centrifuged at 2000 ×*g* for 10 min at 4 °C. The supernatants were then centrifuged at 100,000 ×*g* for 15 min at 4 °C. The final pellets, which contain partially purified membrane fractions, were resuspended in 1 mL of buffer A. Membrane preparations were incubated with adenosine deaminase (1 U/mL) at 37 °C for 15 min to eliminate endogenous adenosine. The concentration of protein was determined by Bradford protein assay (Bradford, 1976) using a standard curve prepared with bovine serum albumin.

Radioligand binding assays

A2AAR, A1AR, and D2R in mouse striatal membranes were quantified using selective radioligands. The A2AAR antagonist ^{125}I 4-(2-[7-amino-2-(2-furyl)[1,2,4]-triazolo[2,3a][1,3,5] triazin-5-ylamino]ethyl)phenol (ZM241385) (2100 Ci/mmol) was generated in our laboratory using ^{125}I Na (PerkinElmer Life and Analytical Science, Billerica, MA) and chloramine T and purified by HPLC (Palmer et al., 1995). Characterization of the binding characteristics of this radioligand is also provided by these investigators. The A1AR antagonist [^{3}H]1,3-dipropyl-8-cyclopentylxanthine (DPCPX) (specific activity=120 Ci/mmol), and the D2R antagonist [^{3}H]methyspiperone (specific activity=90 Ci/mmol) were obtained from PerkinElmer Life and Analytical Science, respectively. Assays were performed by incubating membranes (50 μg protein per tube) at 37 °C for 1 h with the individual radioligands in a total volume of 250 μL or 500 μL (for [^{3}H] methyspiperone binding assay) of 50 mM Tris–HCl buffer (pH 7.4 at 37 °C), containing 10 mM $MgCl_2$, 1 mM EDTA, 10 μg/mL soybean trypsin inhibitor, 10 μg/mL benzamidine, and 2 μg/mL pepstatin. Nonspecific binding was defined by using 1 mM of theophylline to saturate the non-ARs binding sites (for A1 and A2AAR), and 5 μM of butaclamol (for D2R). At the end of incubation, samples were filtered through polyethyleneimine treated (0.05% in de-ionized water) Whatman GF/B glass fiber filters (Whatman, Clifton, NJ) using a cell

harvester (Brandel, Gaithersburg, MD), and quickly washed for 2 times with ice-cold 50 mM Tris–HCl buffer containing 0.01% 3-[(3-cholamidopropyl) dimethyl-ammonio]-1propanesulfonate.

Bound radioactivity was determined using a gamma counter for ^{125}I-ZM 241385 binding, and a liquid scintillation counter for [^{3}H]-DPCPX and [^{3}H]-methyspiperone binding. Specific binding of each sample was obtained by subtraction of non-specific binding from total binding. Saturation curves were generated using a computer-based curve-fitting program with an integrated statistical package (GraphPad Prism, San Diego, CA). Within each assay, samples were processed in triplicate, with the mean value used for subsequent analysis. Each experiment was repeated of a minimum of 3 times.

Reverse transcription of RNA and real time PCR

Total RNA was extracted from mouse striata using the RNeasy Mini Kit (Qiagen Science, Valencia, CA) according to manufacturer's instructions, and was quantified with spectro-photometer. DNA components in RNA extract were eliminated prior to cDNA synthesis by incubating 1 μg of extracted total RNA with 1 μL of DNase at 37 °C for 30 min. EDTA (25 mM, 1 μL) and Oligo (dt) 12–18 primer (1 μL) (Invitrogen, Carlsbad, CA) were then added sequentially and incubated at 65 °C for 10 min and 70 °C for 5 min, respectively. Reverse transcription of total RNA to cDNA was performed by incubating total RNA with 4 μL of 5× RT buffer, 2 μL of DTT (0.1%), 1 μL of 400 μM dNTPs, 1 μL Superscript RNase II H^{-} reverse transcriptase, and 0.5 μL of RNase inhibitor (Invitrogen) at 42 °C for 60 min, followed by 70 °C 15 min. Synthesized cDNA were added with 12.5 μL of SyBGreen supermix (Bio-Rad, Hercules, CA) and 1 μL (10 pM) of mouse AR and D2R primer sets (Integrated DNA Technologies, Coralville, CA) as follows: A1AR: sense: 5′-CAT TGG GCC ACA GAC CTA CT-3′; antisense: 5′-CAA GGG AGA GAA TCC AGC AG-3′; A2AAR: sense: 5′-GAA GCA GAT GGA GAG CCA AC-3′; antisense: 5′-GAG AGG ATG ATG GCC AGG TA-3′; D2R: sense: 5′-CTG GAG AGG CAG AAC TGG AG-3′; antisense: 5′-TAG ACG ACC CAG GGC ATA AC-3′.

The reaction mix for real time PCR was set up as follows: 2 μL of cDNA, 0.5 μL of each primer (50 pM stock) and 12.5 μL of the iQ SYBR Green Supermix reagent (Bio-Rad), adjusted to a total volume of 25 μL with DNAse/RNAse free water. GAPDH was used for normalization. Amplification and detection was performed with the Cepheid Smart Cycler Detection System (Cepheid, Sunnyvale, CA). Negative control reactions for A1AR, A2AAR, D2R and GAPDH were set up as above without any template cDNA. Cycling conditions were: 95 °C for 3 min followed by 50 cycles at 95 °C for 15 s, 64 °C for 30 s and 72 °C for 30 s. On completion of amplification, melting curve analysis was performed by cooling the reaction to 60 °C and then heating slowly to 95 °C, according to the instruction of manufacturer (Cepheid systems). The cycle number at which the sample reaches the threshold fluorescent intensity was termed the cycle threshold (Ct). The relative changes in mRNA levels between F2 and p50 KO striata were measured as [(Ct gene1 − Ct GAPDH1) − (Ct gene2 − Ct GAPDH2)] (Soong et al., 2001). Relative changes in mRNA levels between samples were expressed as a percentage of normal control. Real time PCR products were analyzed on a 2.5% agarose gel to verify the correct product sizes, and the amplified product was visualized using ethidium bromide staining.

Traditional PCR was performed using 1 μL cDNA (prepared as above), 1 μL each of PCR primers, 5 μL 2× Biomix Red (Laboratory Products Sales, Inc. Rochester, NY), in a total volume of 10 μL of H_2O. Each sample was coated on top with mineral oil. PCR were performed with DNA Thermal Cycler 480 (Perkin Elmer Corporation, Norwalk, CT). Cycles include a 5 min denaturation step at 95 °C, followed by 25 cycles each consisting of a 1 min 95 °C denaturing step, 1 min 58 °C annealing step and 2 min 72 °C extension step. PCR products were resolved on 2.5% agarose gels, stained with ethidium bromide solution for 30 min, visualized under a UV source and photographed with digital camera (Gel Logic 200 Imaging System, Eastman Kodak Company, Rochester, NY).

Immunopreciptiation and purification of membrane Ars

Striatal membranes were pooled to accumulate a 1000 μg sample size for each mouse strain. Immunoprecipitation was performed with Seize X Mammalian Immunoprecipitation Kit (Pierce, Rockford, IL) as recommended in the manufacturer's instructions. Briefly, 400 μL of 50% immobilized protein G slurry was added to mini columns (one per strain per AR subtype) prepared in micro-centrifuge tubes, and a gel was built by centrifugation. Fifty μg of A1AR and A2AAR goat polyclonal antibody (Santa Cruz Biotechnology, Santa Cruz, CA) was added respectively to columns, followed by overnight incubation to allow binding of antibodies to gel. Disuccinimidyl suberate (DSS) was then added to cross-link bound antibody. Antigen proteins were extracted by adding lysing buffer to membrane samples. After incubation and centrifugation, 500 μL of supernatants (diluted 1:1 with wash buffer) was again added to columns, followed by a second overnight incubation at 4 °C. AR proteins bound to antibodies on the gel were collected by washing for three times with elution buffer. The three eluted fractions were pooled and were used for iodination and SDS-PAGE.

Iodination and quantification of purified membrane AR protein

Immunopreciptiation purified membrane ARs products were labeled with ^{125}I Na using chloramine T. Samples were then desalted on a G25 Sephadex column, eluted in 10 mM Tris–HCl buffer containing 0.05% CHAPS, and 50,000 cpm of each group was resolved on SDS-PAGE using a 12% acrylamide gel. Gels were heat-dried and autoradiography was performed using Kodak XAR film (Eastman Kodak Company, Rochester, NY). Gel sections corresponding to the receptor bands were removed for quantification of radioactivity.

Western blot for G protein subunits

To quantify the levels of $G_{s\alpha}$, $G_{olf\alpha}$, $G_{i1\alpha}$ and G_{β} proteins, 50 μg of striatal membrane proteins was solubilized in SDS-PAGE buffer and resolved on a 12% polyacrylamide gel.

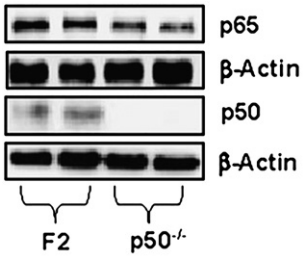


Fig. 1. Expression of NF-κB p50 and p65 subunits in mouse striatum. Striata were processed for Western blotting. Blots were probed with polyclonal antibodies for either p65 or p50, and were normalized using β-actin. The striata of p50 KO mice show bands for p65 but not for p50. Data shown are representative of three individual mice from each strain.

Resolved protein bands were transferred to nitrocellulose membranes, blocked in Blotto buffer (130 mM NaCl, 2.7 mM KCl, 1.8 mM Na_2HPO_4, 1.5 mM KH_2PO_4, 0.1% NaN_3, 0.1% Triton-X 100, and 5% low-fat skim milk) for 1 h, and incubated overnight at 4 °C with the rabbit polyclonal anti-$G_{s\alpha}$, anti-G_{olf}, anti-$G_{i1\alpha}$ and anti-G_{β} common antibodies (Calbiochem, San Diego, CA). Blots were then washed five times with Tris-buffered saline (TBS)/Tween 20 (20 mM Tris–HCl, 137 mM NaCl, 0.1% Tween 20, pH 7.6 at room temperature) and incubated with goat anti-rabbit IgG (Santa Cruz Biotechnology, Santa Cruz, CA) in TBS for 1 h at room temperature. This was followed by 3 washes with TBS (10 min each) and exposed to enhanced chemiluminescence (ECL) reagent (Amersham Biosciences, Picataway, NJ) for visualization. Blots were then exposed to X-ray film exposure for visualization of the protein bands. The nitrocellulose blots were then striped of bound antibodies and treated with rabbit β-actin antibody (1:1000) (Santa Cruz Biotechnology) for normalization.

Immunohistochemistry

Each mouse was anesthetized with near lethal doses of a mixture of ketamine and xylazine. The chest was opened, the descending aorta cut open and a needle was inserted through the right ventricle into the aorta. Perfusion involved sequentially injecting 0.9% saline solution (until the blood was washed out), followed by 4% paraformaldehyde for 2 min. The mouse was then decapitated, whole brain was removed, and stored overnight in a capped vial containing 4% paraformaldehyde. Sagittal sections were carried out in the midline of the mouse brain, and the two hemisections were paraffin-embedded and manually sectioned (10 μm thick) using a microtome. Sections were placed on Vectabond reagent processed glass slides

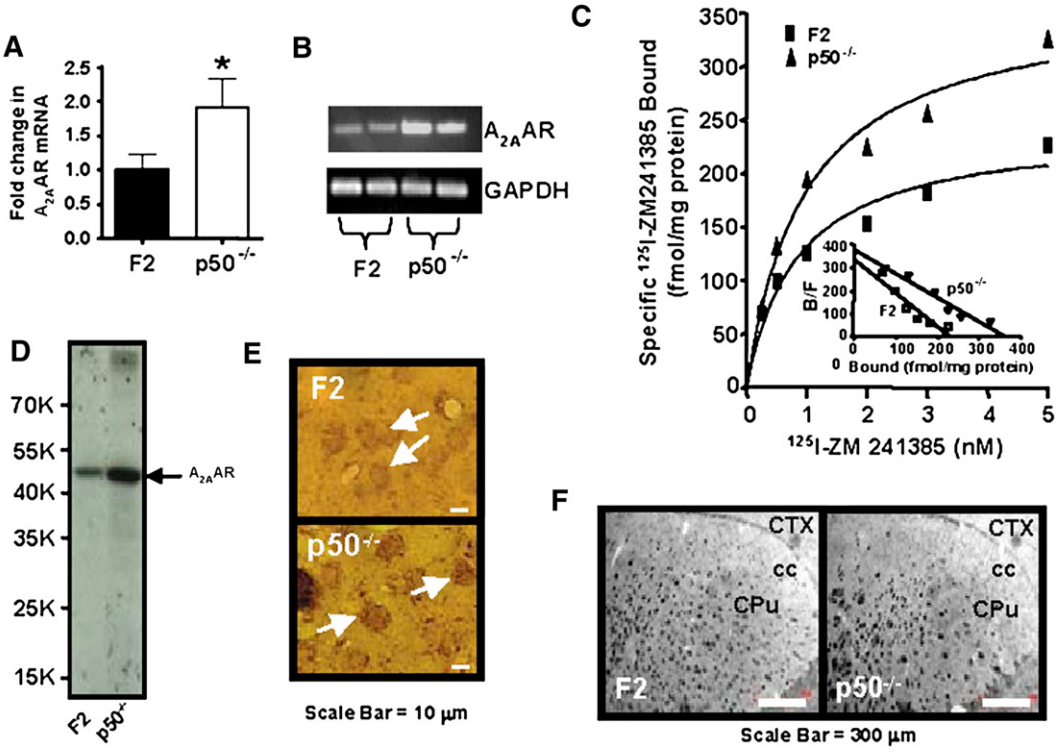


Fig. 2. Increased expression of A2AAR in striata of p50 KO versus F2 mice. Total RNA was prepared and used for real time PCR (A) ($n=10$ mice per group) or traditional PCR ($n=2$ per group) (B). Asterisk (*) in (A) indicates statistical significant difference from F2 mice ($p<0.05$). B, The results of real time PCR of A2AAR mRNA are presented after normalization to GAPDH mRNA. C, Saturation curves for ^{125}I-ZM241385 binding to A2AAR in mouse crude striatal membranes. The plots shown represent pooled striata from 4 mice, with samples at each concentration assayed in triplicate. This analysis was repeated on 3 different pooled samples and yielded similar results. Inset, Scatchard plot . D, Affinity purification of the A2AAR from F2 and p50 KO striata. Four striata per strain were pooled to prepare 1000 μg of tissue for receptor purification, iodination, resolution on SDS-PAGE and visualization by autoradiography. E, Immunohistochemistry of striatal A2AAR from F2 and p50 KO mice ($n=4$ per group). Arrowheads depict specific A2AAR-immunolabeled neurons. The sections represent a 400-fold magnification of the image. Scale bar represents 10 μm. F, Low magnification image of the striatum from F2 and p50 KO mice obtained from the A2AAR immunostained sections showing similar gross morphology. Abbreviations: cc, corpus callosum; CPu, caudate putamen; CTX, cortex.

(Vector Laboratories, Burlingame, CA) and air-dried overnight at room temperature. Sections were then dipped in xylene (3 washes), followed by decreasing concentrations (100, 95 and 70%) of ethanol. Immunohistochemistry for A1AR and A2AAR was performed using a VectaStain Elite ABC kit (Vector Laboratories) according to the manufacturer's instruction. Briefly, sections were soaked in 0.3% hydrogen peroxide solution for 30 min, incubated for 1 h in blocking buffer, and then incubated overnight (at 4 °C) with A1AR or A2AAR antibodies (Santa Cruz Biotechnology) at dilution of 1: 150 in PBS. Sections were incubated with biotinylated secondary antibody for 1 h and for 30 min in VectaStain Elite ABC reagent (A and B). The sections were incubated in mixed solution prepared from diaminobenzadine (DAB) substrate kit for 5 min, rinsed with water, dehydrated through alcohol into xylene and mounted with permount.

For microscopic examination, images were captured with a digital camera (Microshot, Nikon, 40× objective) from fields in the central striatal area of each section (the region with major distribution of neuronal fiber bundle), and 30–35 stained neurons from 6–9 fields out of 4 samples were selected for density measurement using a computer analysis program (Microcomputer Imaging Device, Imaging Research Inc., St. Catherines, Ontario, Canada). Neuronal density was expressed as the ratio of pixels to defined area, and was normalized against background density of each field. Mean values were obtained for between-strain comparisons.

Cresyl violet staining was performed on adjacent sections using 2.0 g/L of cresyl violet (Sigma-Aldrich) for 5 min. The sections were rinsed with water, then acidified 95% ethanol, rinsed in water and then dehydrated with increasing concentrations of ethanol (70–100%), followed by xylene rinses. Sections were mounted on glass slides using Permount and allowed to dry overnight. Imaging was performed using an Olympus Optical system (Mellville, NY).

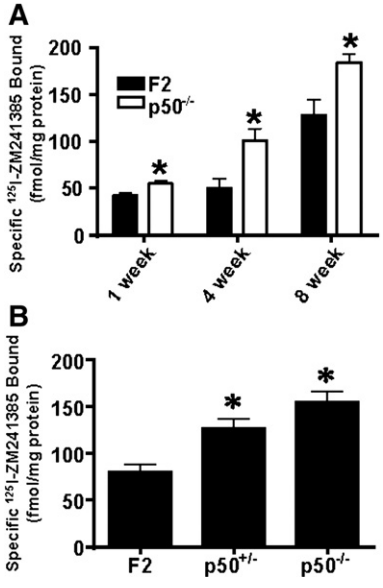


Fig. 3. Developmental profile and gene dose effect on A2AAR binding in striata of p50 KO and F2 mice. A, Striata were obtained from F2 and p50 KO mice that were sacrificed at 1, 4 and 8 weeks of age ($n=5$ per group). Radioligand binding assays were performed using the ligand ^{125}I-ZM241385 (1 nM). B, ^{125}I-ZM241385 binding in striata of 2-month old F2, heterozygous p50 KO and homozygous p50 KO mice ($n=6$ per group). Asterisk (*) indicate statistical significant difference from F2 mice ($p<0.05$).

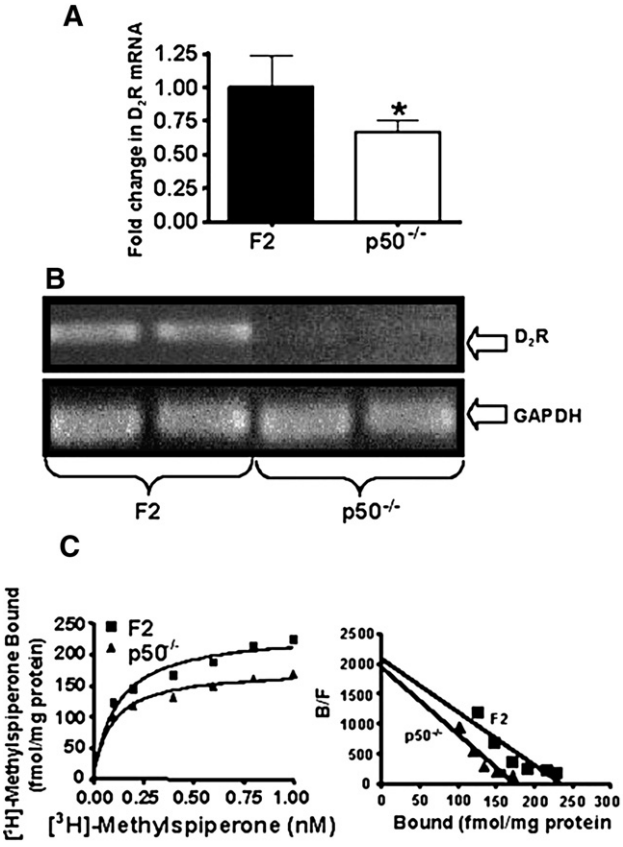


Fig. 4. Reduced expression of D2R in striatum of the p50 KO versus F2 mice. Total striatal RNA was prepared and used for real time ($n=10$ per group) (A) and traditional PCR ($n=2$ per group) (B). The results of traditional PCR of D2R mRNA are shown with the respective GAPDH mRNA used for normalization. Real time data show a significant reduction in D2R mRNA in striata obtained from p50 KO mice compared to F2 controls ($p<0.05$ as indicated by asterisk). (C) Saturation plots for [^{3}H]-methylspiperone binding to D2R mouse crude striatal plasma membranes. The plots shown represent pooled striata from 4 mice, with samples at each concentration assayed in triplicate. This analysis was repeated on 3 different pooled samples and yielded similar results. Scatchard plot of the data is shown on the right.

Statistical analysis

Statistical differences among groups were evaluated by one-way and two-way analysis of variance (ANOVA) with post hoc Tukey analyses using SPSS software (SPSS Inc., Chicago, IL). All data are presented as mean ± standard error. B_{max} and K_d values were obtained from saturation curves by non-linear regression analysis using GraphPad Prism software.

Results

To validate that absence of the protein in p50 KO mice, we used Western blotting to measure the protein in striatum. The p50 protein was present in F2 mice, but was not detectable in

striata of p50 KO mice (Fig. 1). The p65 protein was detected in both strains, and did not change significantly when the lanes were normalized to the levels of β-actin in this or our previous study (Jhaveri et al., 2007).

Striatal A2AAR in p50 KO versus F2 mice

Analysis of the steady-state levels of A2AAR mRNA using real time PCR revealed significantly higher levels in the striata of p50 KO mice (1.9±0.4 fold) as compared with F2 mice ($p<0.05$) (Fig. 2B). Real time PCR data were validated by traditional PCR; the predicted 207 bp products were visualized on an agarose gel stained with ethidium bromide. Analysis of the ethidium bromide-stained gels showed 1.6±0.2 fold more A2AAR mRNA in striata of p50 KO versus F2 mice (Fig. 2B).

Single point binding using the selective A2AAR antagonist ZM241385 (1 nM) revealed significantly higher A2AAR binding in p50 KO mice than in F2 mice ($p<0.05$). Values for F2 and p50 KO mice were 54±8 and 135±28 fmol/mg protein, respectively. Similar findings were obtained using the selective A2AAR agonist CGS21680 (data not shown). Scatchard analyses revealed that the total number of receptors (B_{max}) was significantly higher in p50 KO mice than in F2 mice ($p<0.01$) (Fig. 2C, inset). B_{max} values were 245±7 and 365±30 fmol/mg protein in F2 and p50 KO mice, respectively. The equilibrium dissociation constants (K_d) were not significantly different between mouse strains. The respective K_d values were 0.88±0.20 and 1.02±0.14 nM. The increase in A2AAR protein expression was confirmed by quantification of the A2AAR immunopurified from the striata of p50 KO and F2 mice. Iodination of these preparations and resolution on SDS-PAGE indicate average ^{125}I incorporation of 1980 cpm and 496 cpm (mean of 2 experiments) from p50 KO and F2 mice, respectively (Fig. 2D). Further confirmation of increased A2AAR expression was demonstrated by immunohistochemistry (Fig. 2E), which showed greater labeling of striatal neurons in the p50 KO mice ($p<0.01$). The average density of specific A2AAR-immunostained striatal neurons was 3.5±0.3 fold greater in the striata of p50 KO mice, as compared to the F2 mice. Regional differences in A2AAR staining (data not shown) and gross structural differences in morphology of adjacent cresyl violet-stained sections were not observed in comparing the striata of F2 and p50 mice, using low power magnification (Fig. 2F).

To determine whether the elevation in A2AAR protein expression developed as a function of age, we performed radioligand binding studies in striata from F2 and p50 KO mice at 1, 4 and 8 weeks of age. In all three age groups, ^{125}I-ZM241385 binding was significantly greater in p50 KO versus F2 mice ($p<0.05$ for between-strain comparison of 1, 4, and 8 week old

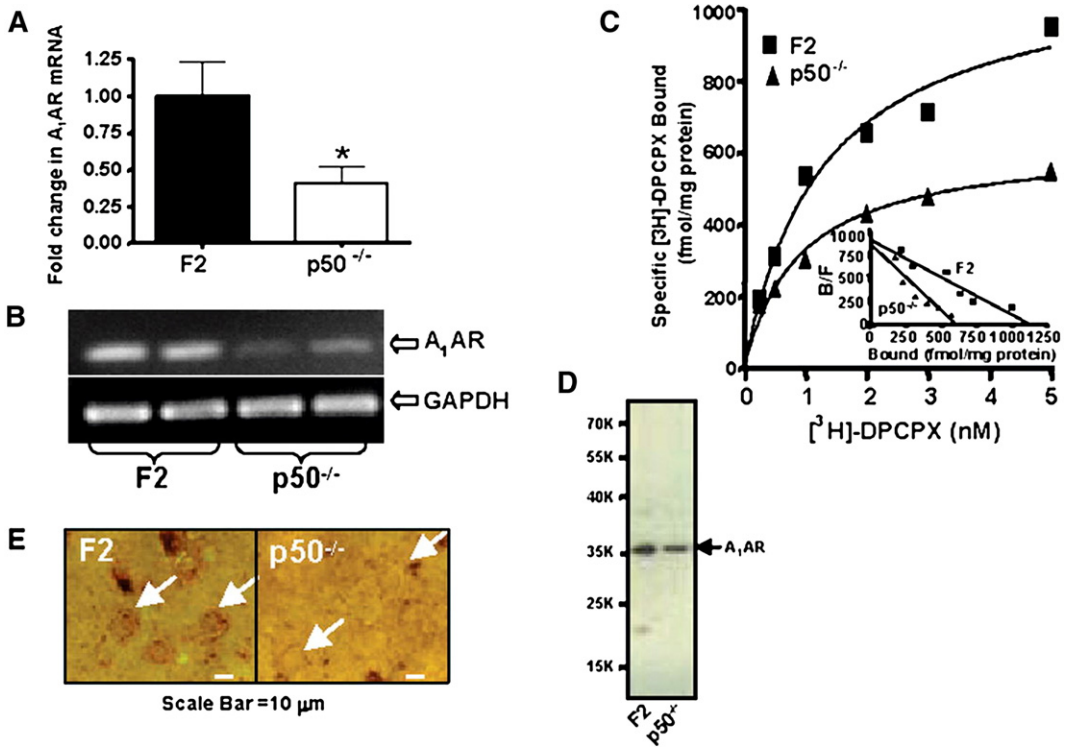


Fig. 5. Expression of A1AR in striata of p50 KO and F2 mice. Total striatal RNA was prepared and used for real time ($n=10$ per group) (A) and traditional PCR ($n=2$ per group) (B). The results of real time PCR of A1AR mRNA are shown as the mean±SEM, after normalization to GAPDH mRNA. Asterisk (*) indicate statistical significance from the F2 mice ($p<0.05$). C, Saturation curves for [^{3}H]-DPCPX binding to the A1AR in mouse crude striatal plasma membranes. The plots shown represent pooled striata from 4 mice, with samples at each concentration assayed in triplicate. This analysis was repeated on 3 separate pooled samples, and each provided similar results. Inset, Scatchard plot of the data. D, Affinity purification of the A1AR from mouse striatum. Four striata per strain were pooled to prepare 1000 μg of protein for receptor purification, iodination, resolution on SDS-PAGE and visualization of the dried gel using Kodak XAR film. E, Immunohistochemistry of striatal A1AR from F2 and p50 KO mice ($n=4$ per group). Specific A1AR-immunolabeled neurons are depicted by arrowheads. These sections represent a 400-fold magnification of the image. Scale bar represents 10 μm.

mice) (Fig. 3A). Specific binding for the three groups were 43±3, 51±10 and 129±13 fmol/mg protein and 56±3, 102±11 and 185±9 fmol/mg protein for F2 and p50 KO animals, respectively.

To determine whether the increased A2AAR phenotype was evident in heterozygous p50 KO mice, male p50 KO mice were bred with female F1 mice. Mice were sacrificed at 8 weeks of age, and striata were removed and used for radioligand binding studies. Binding of ^{125}I-ZM 241385 was higher in striata of p50 KO homozygous and heterozygous mice, as compared with the F2 mice ($p<0.05$). However, binding did not differ significantly between the heterozygous and homozygous KO mice ($p>0.05$) (Fig. 3B). A2AAR binding in the striata of F2, heterozygous KO and homozygous KO mice were 82±3, 129±16 and 156±11 fmol/mg protein, respectively ($p<0.05$).

D2R in striatum of p50 KO versus F2 mice

D2R mRNA was significantly lower in p50 KO mice (0.7±0.1 fold of F2 values; $p<0.01$), as indicated by real time PCR (Fig. 4A). Analysis of the ethidium stained gels from traditional PCR also showed less D2R expression (product size 242 bp) in striata of p50 KO mice (Fig. 4B). Single point binding using the selective D2R antagonist methyspiperone showed significantly less D2R binding in p50 KO than in F2 mice (51±3 and 26±3 fmol/mg protein for F2 and p50 KO mice, respectively; $p<0.01$). Scatchard plots of saturation data revealed significantly lower B_{max} values in p50 KO mice as compared with F2 mice ($p<0.01$), with no change in K_d values (Fig. 4C, right side). The B_{max} values for striatal [^{3}H]-methylspiperone binding were 240±12 and 175±6 fmol/mg protein for F2 and p50 KO mice, respectively. The respective K_d values were 0.12±0.02 and 0.09±0.01 nM.

A1AR in striatum of p50 KO versus F2 mice

Quantification of A1AR mRNA by real time PCR revealed significantly less A1AR mRNA in striatum of p50 KO mice as compared with the F2 mice (0.4±0.1 fold; $p<0.01$) (Fig. 5A). This difference was confirmed by using ethidium bromide-stained gels, which revealed the 200 bp product obtained by

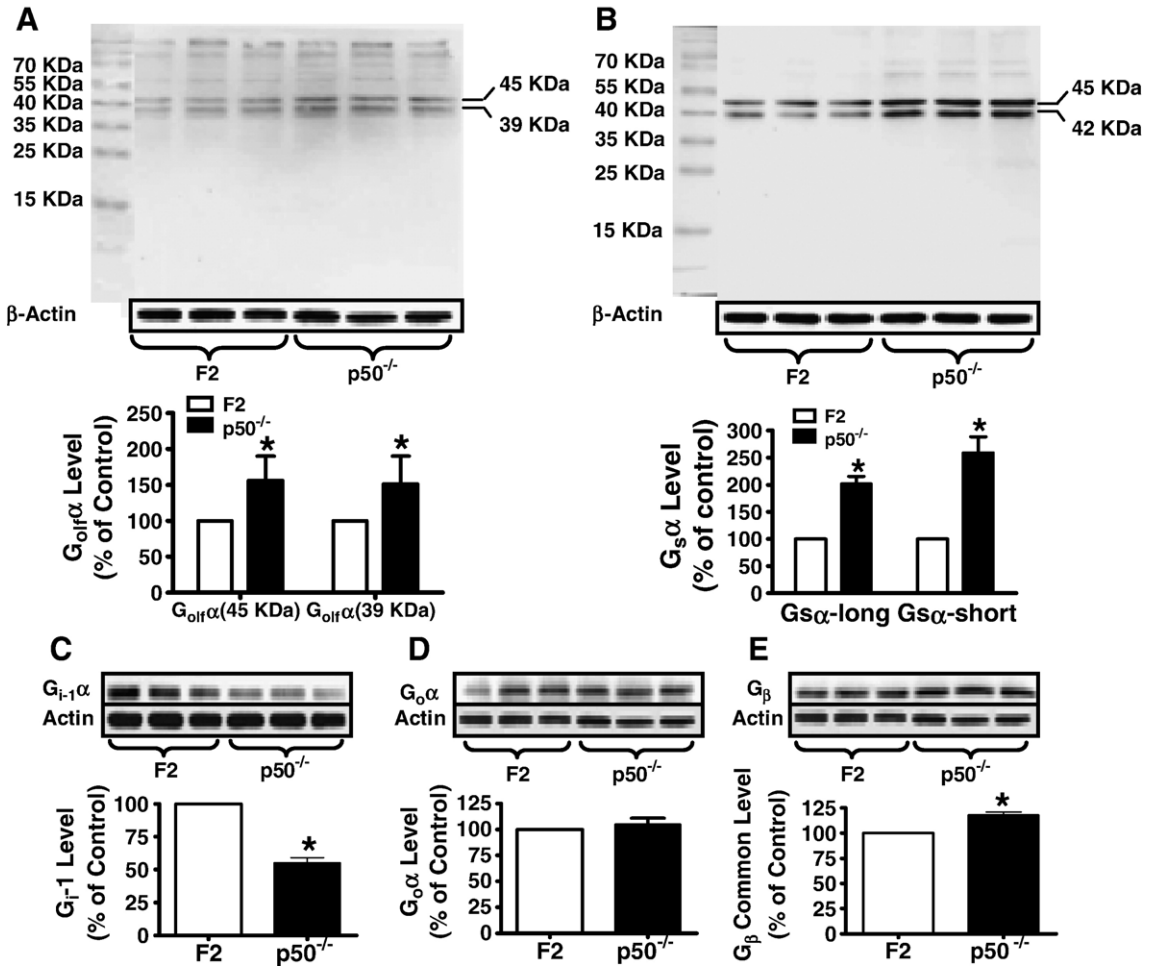


Fig. 6. Differential regulation of striatal G protein α and β subunits in p50 KO versus F2 mice. Crude striatal plasma membranes were prepared ($n=4$ per group), solubilized in SDS-PAGE buffer and resolved on a 12% polyacrylamide gel. Western blotting was performed using rabbit polyclonal G_α and G_β antibodies, and the protein bands were visualized using a goat anti-rabbit IgG linked to horseradish peroxidase. The bands were normalized the levels of β-actin detected on the same gel. Western blots and the levels of the $G_{olf\alpha}$, $G_{\alpha s}$, $G_{\alpha i1}$, $G_{\alpha o}$ and G_β are shown in panels A–E, respectively. Quantification of the data is shown in bar graphs. The stained left lanes in A and B represent the molecular weight markers. Asterisks indicate a significant difference from F2 mice ($p<0.05$).

traditional PCR (band intensity in p50 KO mice was 0.6±0.1 fold of F2 intensity) (Fig. 5B). Single point binding using the selective A1AR antagonist DPCPX (1 nM) revealed significantly less A1AR binding in p50 KO mice as compared with F2 mice (322±11 and 129±37 fmol/mg protein for F2 and p50 KO mice, respectively; $p<0.01$). Scatchard analysis of saturation data revealed significantly lower B_{max} values in p50 KO than in F2 mice (B_{max} values of 1182±130 and 632±39 fmol/mg protein for F2 and p50 KO mice, respectively; $p<0.01$) (Fig. 5C). The respective K_d values were 1.57±0.6 and 0.94±0.20 nM.

The decrease in A1AR was confirmed by immunopurification of the A1AR, followed by iodination, and resolution of the iodinated protein by SDS-PAGE. Excision and quantification of the radioactive band showed less ^{125}I incorporation into the A1AR of p50 KO mice (mean value=1575 cpm) than into F2 mice (mean value=2335 cpm) (Fig. 5D). Furthermore, quantification of striatal neurons that stained positively with the A1AR polyclonal antibody demonstrated less immunolabeling in p50 KO mice compared with F2 animals ($p<0.01$) (Fig. 5E). The average staining density of specific A1AR-immunostained striatal neurons was 0.64±0.1 fold in p50 mice, as compared with the F2 mice ($p<0.01$) (Fig. 5E).

Differential expression of G protein subunits in striatum of p50 KO versus F2 mice

$G_{olf\alpha}$ protein was detected as two prominent bands at 45 kDa and 39 kDa in striata of both F2 and p50 KO mice. The 45 and 39 kDa bands of p50 KO mice were 156±34% and 151±39%, respectively, of F2 mice ($n=3$, $p<0.05$) (Fig. 6A). Western blotting revealed similar changes in the expression of the $G_{s\alpha}$ proteins, with p50 KO values of 152±15% and 203±19% of F2 values for $G_{s\alpha}$ short (~42 kDa) and long (~45 kDa) isoforms, respectively ($p<0.05$) (Fig. 6B). In contrast, the levels of the striatal $G_{i1\alpha}$ protein in p50 KO mice were reduced to 55±4% of the F2 values (Fig. 6C). $G_{o\alpha}$ protein levels did not differ between the two strains (Fig. 6D). However, p50 KO mice had more striatal G_{β} subunit (118±3%; $n=3$, $p<0.05$) than did F2 mice (Fig. 6E).

Response of p50 KO and F2 mice to caffeine

Multi-factoral analysis was performed to determine the influence of factors included in the study on activity levels elicited under current experimental conditions. The between subject factor was mouse strain (F2 and p50 KO mice), and the

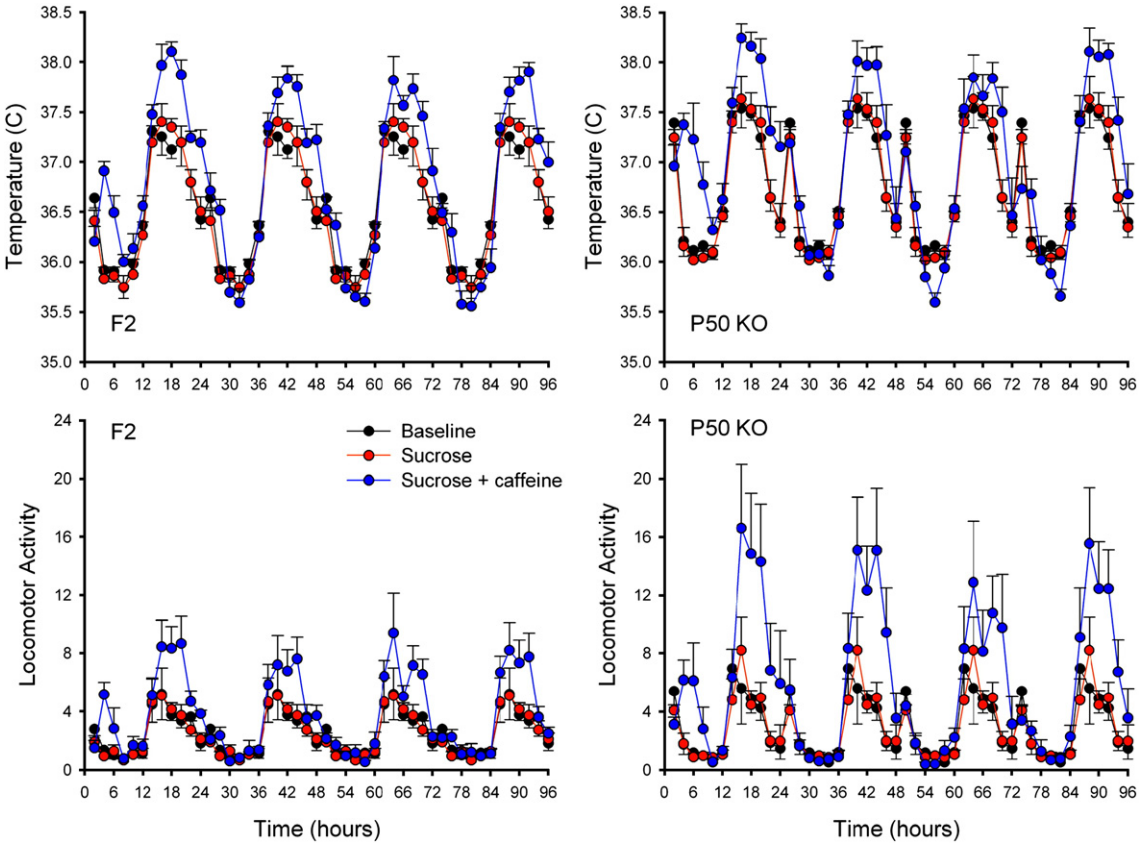


Fig. 7. Response of p50 KO and F2 mice to caffeine ingestion. Mice of both strains were randomly assigned into caffeine treatment or control groups ($n=14$ per group). Caffeine was administered in drinking water (300 mg/L) in combination with sucrose (20 g/L). Control groups received only sucrose (20 g/L) in drinking water. Mice received sequentially regular drinking water for 48 h (baseline), sucrose only in drinking water for the next 48 h, and caffeine with sucrose for the final 96 h. Locomotor activity in the light and dark phases showed no between-strain difference during baseline and sucrose treatments, but p50 KO mice showed greater locomotor activity that did F2 mice during the dark phases in response to caffeine ingestion.

within subject factors were treatment (regular water, sucrose, and sucrose plus caffeine), observation phase (light and dark), observation interval (2 days for regular water, 2 days for sucrose, and 4 days for caffeine), and specific 2-h averages. The period of caffeine treatment was divided into two sub-sections (*i.e.*, days 1–2 and 3–4 of caffeine treatment). Under non-caffeine conditions, both strains showed comparable amounts and diurnal patterns of locomotor activity, and activity did not vary significantly as a function of water or sucrose treatment ($p>0.9$). Activity was also equivalent during the two caffeine treatment intervals ($p>0.08$). Combining the water and sucrose data into a "non-caffeine" group for comparison with the four days of caffeine treatment revealed a tendency of higher activity level in p50 KO versus F2 mice in the dark phase, but not in the light phase ($p=0.061$). Subsequent step-down analysis using only the dark phase data revealed significantly increased activity in both strains in response to caffeine treatment ($p<0.001$). Furthermore, as compared with F2 mice, p50 KO mice showed a significantly greater behavioral activation in response to caffeine ingestion ($p=0.041$). In contrast to activity, temperature responses after caffeine ingestion were similar in both strains of mice (Fig. 7).

Discussion

Data presented here show that p50 KO mice have greater striatal A2AAR and less D2R and A1AR than do genetically intact F2 mice. In addition, p50 KO mice have higher striatal $G_{\alpha olf}$, $G_{\alpha s}$ and G_{β} proteins but lower amounts of $G_{\alpha i1}$ protein. Moreover, the p50 KO mice show greater behavioral activation in response to caffeine ingestion than do F2 mice.

Our data provide *in vivo* support for NF-κB/p50-mediated suppression of striatal A2AAR expression in mice. In a previous report (Nie et al., 1999), we showed that NGF suppression of A2AAR expression in PC12 cells was mediated via NF-κB and speculated on a role for the p50/p50 homodimer in mediating transcriptional inhibition. Based on that *in vitro* study and the current data, we propose that the greater amount of A2AAR mRNA present in striata of p50 KO mice could reflect disinhibition of A2AAR expression due to altered NF-κB function. The p50 subunit acts as a transcriptional inhibitor of interleukin-2 (IL-2) expression in non-transformed CD4+ T lymphocyte clones (Kang et al., 1992). Basal expression of IL-2 is mediated by the p50/p50 homodimer, whereas induction of IL-2 by antigenic stimulation results in reduced p50/p50 homodimer and increased p50/p65 levels (Kang et al., 1992). The current data showing enhanced expression of the A2AAR in striatum of p50 KO mice provides indirect support for a similar mechanism underlying the regulation of the A2AAR. Accordingly, the lack of the p50 subunit will remove the suppression of A2AAR transcription mediated by the p50/p50 homodimer. Although the p50 protein was undetectable in striata from $p50^{-/-}$ mice as compared with F2 mice, p65 protein did not change significantly when the lanes were normalized to the levels of β-actin in this and our previous study (Jhaveri et al., 2007). An alternative possibility is that the changes in receptor proteins are correlated with but not directly caused by a loss of NF-κB function.

A2AAR and D2R co-localize on GABAergic striatopallidal neurons, where they mediate reciprocal inhibitory actions (Xu et al., 2005). Increased A2AAR was present in p50 KO mice at as early as 1 week of age. This finding suggests that NF-κB could regulate A2AAR synthesis during ontogeny, with a deficit in the p50 subunit leading to enhanced production. A2AAR binding in striatum of did not differ between homozygous and heterozygous p50 KO mice, although binding in both was higher than in F2 mice.

In addition to the A2AAR, levels of both the long and short forms of the $G_{\alpha s}$ and $G_{\alpha olf}$ proteins, which transduce receptor activation to stimulate adenylyl cyclase activity, were greater in p50 KO mice than in F2 mice. An increased G_s/G_{olf} protein level would contribute to increased receptor-mediated $G_{\alpha s}/G_{\alpha olf}$ activation and therefore to increased adenylyl cyclase activity (Kukkonen et al., 2001). Either of the two isoforms of $G_{\alpha s}$ protein can initiate activation of adenylyl cyclase (Graziano et al., 1987). Because the activity of $G_{\alpha s}$ and $G_{\alpha olf}$ protein-coupled receptors depends on the extent of G protein coupling, the coordinated upregulation of A2AAR and $G_{\alpha s}$ and $G_{\alpha olf}$ proteins in the p50 KO mice would amplify downstream signaling. The increased striatal $G_{\alpha s}$ and $G_{\alpha olf}$ is also consistent with a tonic inhibitory action of NF-κB on the expression of this protein *in vivo*. In contrast, the level of $G_{\alpha i1}$ was significantly reduced, possibly in compensation for increased $G_{\alpha s}$ and $G_{\alpha olf}$ and the A2AAR. Accordingly, this could lead to diminished signaling via the A1AR and D2R (see below) which use this inhibitory G protein.

Our data show that the striatal expression of A1AR mRNA and protein is lower in the p50 KO mice as compared with the F2 controls, suggesting both that the absence of p50 reduces transcription of A1AR in the p50 KO mice and that NF-κB regulates A1AR expression *in vivo* under normal conditions. Several lines of evidence further support the latter possibility. For example, an NF-κB consensus sequence located 623 bp upstream of the promoter A transcription start site mediates the induction of A1AR by oxidative stress (Nie et al., 1998). In addition, challenge with various cytotoxic agents, including cisplatin and anthracyclines, increases A1AR expression and promoter activity through activation of NF-κB (Nie et al., 1998). Induction of A1AR expression by cisplatin, possibly mediated via NF-κB, also occurs in the chinchilla cochlea (Ford et al., 1997) and in the rat kidney (Bhat et al., 2001). In addition, NF-κB has been implicated in the induction of A1AR in the cochlea in response to noise exposure (Ramkumar et al., 2004), and in basal forebrain in response to sleep deprivation (Basheer et al., 2001). However, alternative mechanisms for reduced A1AR in p50 KO mice are also feasible. For example, the lower amount of A1AR protein could reflect reduced stability of A1AR mRNA in the p50 KO mice. Another possibility is impaired transport and insertion of the A1AR into the plasma membrane in the absence of p50. However, our observation that membrane expression of the A2AAR and $G_{s\alpha}/G_{olf\alpha}$ proteins is increased in p50 KO mice implies absence of a generalized defect in membrane targeting of proteins in these mice. Striatal A1ARs are localized primarily on intrinsic striatal neurons and on corticostriatal afferents rather than on dopaminergic afferents

(Alexander and Reddington, 1989; Quarta et al., 2004). A1AR are also present on striatal GABAergic and cholinergic neurons (Ferre et al., 1996). Activation of striatal A1AR reduces dopamine and acetylcholine release (Jin et al., 1993), and negatively affects D1 dopamine receptor neurotransmission (Fuxe et al., 1998).

Striatal D2R expression was also lower in p50 KO mice, as determined by D2R mRNA and binding of the antagonist [^{3}H]-methylspiperone. A previous *in vitro* study also suggested the involvement of NF-κB in the regulation of D2R expression (Fiorentini et al., 2002). Our data support a role for the intact NF-κB in mediating the expression of this D2R *in vivo* under normal conditions. Interestingly, D2R mediates activation of NF-κB (Takeuchi and Fukunaga, 2003) and could therefore promote the expression of proteins, including itself, that depend on this transcription factor. Accordingly, a reduction in D2R would then reduce NF-κB activity and consequently alter the expression of NF-κB-regulated proteins (*e.g.*, D2R, A1AR and A2AAR). Thus, the alterations in striatal expression of these three receptors in p50 KO mice could reflect the combined dysregulation of NF-κB and altered receptor-dependent modulation of NF-κB.

Differential regulation of the A2AAR and D2R and their G proteins would disrupt the normal inhibitory interaction between these two receptor subtypes in the striatum. Accordingly, signaling via the A2AAR will be enhanced while that mediated by the D2R will be reduced. How these changes would affect A2AAR/D2R heterodimer formation (Hillion et al., 2002) is not clear. However, the behavioral consequences of the receptor differences were quite significant. Increased locomotor activity induced by caffeine is viewed to be largely dependent on blockade of striatal A2AAR (Fredholm et al., 1999), suggesting that increased expression of these receptors will provide a larger target for inhibition by caffeine, leading to the observed increase in activity in the p50 KO mice.

Conclusions

In summary, our data show altered characteristics in striatal adenosine and dopamine receptors in mice lacking the p50 subunit of NF-κB. This study is the first to use an NF-κB loss-of-function rodent model to document a modulatory role of NF-κB on the homeostasis of these receptors in striatum. These data provide *in vivo* validation of a critical role for NF-κB in regulating the expression of these receptor proteins in striatum and the behavioral response to drug challenge. In addition, our data highlight the intricate mechanisms underlying regulation of these receptors *in vivo*.

Acknowledgements

The authors thank Lisa Cox, Joel Reichensperger, and the SIUSOM Division of Laboratory Animal Medicine for their technical assistance. This work was supported by National Institute of Health grant RR017543 and the Excellence in Academic Medicine program of the SIU School of Medicine.

References

Alexander, S.P., Reddington, M., 1989. The cellular localization of adenosine receptors in rat neostriatum. Neuroscience 28, 645–651.

Basheer, R., Rainnie, D.G., Porkka-Heiskanen, T., Ramesh, V., McCarley, R.W., 2001. Adenosine, prolonged wakefulness, and A_1-activated NF-kB DNA binding in the basal forebrain of the rat. Neuroscience 104, 731–739.

Beg, A.A., Sha, W.C., Bronson, R.T., Ghosh, S., Baltimore, D., 1995. Embryonic lethality and liver degeneration in mice lacking the RelA component of NF-κB. Nature 376, 167–170.

Bhat, S.G., Mishra, S., Mei, Y., Nie, Z., Whitworth, C.A., Rybak, L.P., Ramkumar, V., 2001. Cisplatin up-regulates the adenosine A1 receptor in the rat kidney. European Journal of Pharmacology 442, 251–264.

Bradford, M.M., 1976. A rapid and sensitive method for the quantitation of microgram quantities of protein utilizing the principle of protein-dye binding. Analytical Biochemistry 72, 248–254.

Dunwiddie, T.V., Masino, S.A., 2001. The role and regulation of adenosine in the central nervous system. Annual Review of Neuroscience 24, 31–55.

Ferre, S., O'Connor, W.T., Svenningsson, P., Bjorklund, L., Lindberg, J., Tinner, B., Stromberg, I., Goldstein, M., Ogren, S.O., Ungerstedt, U., Fredholm, B.B., Fuxe, K., 1996. Dopamine D1 receptor-mediated facilitation of GABAergic neurotransmission in the rat strioentopenduncular pathway and its modulation by adenosine A1 receptor-mediated mechanisms. European Journal of Neuroscience 8, 1545–1553.

Fiorentini, C., Guerra, N., Facchetti, M., Finardi, A., Tiberio, L., Schiaffonati, L., Spano, P., Missale, C., 2002. Nerve growth factor regulates dopamine D2 receptor expression in prolactinoma cell lines via p75-NGFR-mediated activation of nuclear factor-κB. Molecular Endocrinology 16, 353–366.

Ford, M.S., Nie, Z., Whitworth, C.A., Rybak, L.P., Ramkumar, V., 1997. Up-regulation of adenosine receptors in the cochlea by cisplatin. Hearing Research 111, 143–152.

Fredholm, B.B., Bättig, K., Holmen, J., Nehlig, A., Zvartau, E.E., 1999. Actions of caffeine in the brain with special reference to factors that contribute to its widespread use. Pharmacological Reviews 51, 83–133.

Fuxe, K., Ferre, S., Zoli, M., Agnati, L.F., 1998. Integrated events in central dopamine transmission as analyzed at multiple levels. Evidence for intramembrane adenosine A2A/dopamine D2 and adenosine A1/dopamine D1 receptor interactions in the basal ganglia. Brain Research Reviews 26, 273–2588.

Graziano, M.P., Casey, P.J., Gilman, A.G., 1987. Expression of cDNAs for G proteins in *Escherichia coli*. Two forms of $G_{s\alpha}$ stimulate adenylate cyclase. Journal of Biological Chemistry 262, 11375–11381.

Hillion, J., Canals, M., Torvinen, M., Casado, V., Scott, R., Terasmaa, A., Hansson, A., Watson, S., Olah, M.E., Mallol, J., Canela, E.I., Zoli, M., Agnati, L.F., Ibanez, C.F., Lluis, C., Franco, R., Ferre, S., Fuxe, K., 2002. Coaggregation, cointernalization, and codesensitization of adenosine A2A receptors and dopamine D2 receptors. Journal of Biological Chemistry 277, 18091–18097.

Jhaveri, K.A., Reichensperger, J., Toth, L.A., Sekino, Y., Ramkumar, V., 2007. Reduced basal and lipopolysaccharide-stimulated adenosine A1 receptor expression in the brain of nuclear factor-kappaB p50−/− mice. Neuroscience 146, 415–426.

Jin, S., Johansson, B., Fredholm, B.B., 1993. Effects of adenosine A1 and A2 receptor activation on electrically evoked dopamine and acetylcholine release from rat striatal slices. Journal of Pharmacology and Experimental Therapeutics 267, 801–808.

Kang, S.M., Beverly, B., Tran, A.C., Brorson, K., Schwartz, R.H., Lenardo, M.J., 1992. Transactivation by AP-1 is a molecular target of T cell clonal anergy. Science 257, 1134–1138.

Karin, M., Ben-Neriah, Y., 2000. Phosphorylation meets ubiquitination: the control of NF-κB activity. Annual Review of Immunology 18, 621–663.

Kukkonen, J.P., Nasman, J., Akerman, K.E., 2001. Modelling of promiscuous receptor-Gi/Gs protein coupling and effector response. Trends in Pharmacological Sciences 22, 616–622.

Majumdar, S., Mallick, B.N., 2003. Increases levels of tyrosine hydroxylase and glutamic acid decarboxylase in locus coeruleus neurons after rapid eye movement sleep deprivation in rats. Neuroscience Letters 338, 193–196.

Nie, Z., Mei, Y., Ford, M., Rybak, L., Marcuzzi, A., Ren, H., Stiles, G.L., Ramkumar, V., 1998. Oxidative stress increases A_1 adenosine receptor expression by activating nuclear factor kB. Molecular Pharmacology 53, 663–669.

Nie, Z., Mei, Y., Malek, R.L., Marcuzzi, A., Lee, N.H., Ramkumar, V., 1999. A role of p75 in NGF-mediated down-regulation of the A_{2A} adenosine receptors in PC12 cells. Molecular Pharmacology 56, 947–954.

Palmer, T.M., Poucher, S.M., Jacobson, K.A., Stiles, G.L., 1995. 125I-4-(2-[7-amino-2-[2-furyl][1,2,4]triazolo[2,3-a][1,3,5] triazin-5-yl-amino]ethyl)phenol, a high affinity antagonist radioligand selective for the A2a adenosine receptor. Molecular Pharmacology 48, 970–974.

Quarta, D., Borycz, J., Solinas, M., Patkar, K., Hockemeyer, J., Ciruela, F., Lluis, C., Franco, R., Woods, A.S., Goldberg, S.R., Ferre, S., 2004. Adenosine receptor-mediated modulation of dopamine release in the nucleus accumbens depends on glutamate neurotransmission and *N*-methyl-D-aspartate receptor stimulation. Journal of Neurochemistry 91, 873–880.

Ramkumar, V., Whitworth, C.A., Pingle, S.C., Hughes, L.F., Rybak, L.P., 2004. Noise induces A1 adenosine receptor expression in the chinchilla cochlea. Hearing Research 188, 47–56.

Riberio, J.A., Sebastiao, A.M., de Mendonca, A., 2002. Adenosine receptors in the nervous system: pathophysiological implications. Progress in Neurobiology 68, 377–392.

Rosin, D.L., Hettinger, B.D., Lee, A., 2003. Anatomy of adenosine A2A receptors in brain: morphological substrates for integration of striatal function. Neurology 61, S12–S18.

Sands, W.A., Martin, A.F., Strong, E.W., Palmer, T.M., 2004. Specific inhibition of NF-κB dependent inflammatory responses by cell type-specific mechanisms upon A2A adenosine receptor gene transfer. Molecular Pharmacology 66, 1147–1159.

Sha, W.C., Liou, H.C., Toumanen, E.I., Baltimore, D., 1995. Targeted disruption of the p50 subunit of NF-κB leads to multifocal defects in immune responses. Cell 80, 321–330.

Soong, R., Beyser, K., Basten, O., Kalbe, A., Rueschoff, J., Tabiti, K., 2001. Quantitative reverse transcription-polymerase chain reaction detection of cytokeratin 20 in noncolorectal lymph nodes. Clinical Cancer Research 7, 3423–3429.

Takeuchi, Y., Fukunaga, K., 2003. Differential regulation of NF-κB, SRE and CRE by dopamine D1 and D2 receptors in transfected NG108-15 cells. Journal of Neurochemistry 85, 729–739.

Xu, K., Bastia, E., Schwarzschild, M., 2005. Therapeutic potential of adenosine A2A receptor antagonists in Parkinson's disease. Pharmacology & Therapeutics 105, 267–310.

Yu, Z., Zhou, D., Bruce-Keller, A.J., Kindy, M.S., Mattson, M.P., 1999. Lack of the p50 subunit of nuclear factor-κB increases the vulnerability of hippocampal neurons to excitotoxic injury. Journal of Neuroscience 19, 8856–8865.

Yu, Z., Zhou, D., Cheng, G., Mattson, M.P., 2000. Neuroprotective role for the p50 subunit of NFκB in an experimental model of Huntington's disease. Journal of Molecular Neuroscience 15, 31–44.